

Magnetic resonance based morphometric analysis of the tentorial notch

F.J. Arrambide-Garza^{1*} , O. De-La-Garza-Castro^{1*} , L.A. Alvarez-Lozada¹ ,
E. Carranza-Rodriguez² , A. Quiroga-Garza¹ , A. Gomez-Sanchez¹ ,
R. Pinales-Razo² , R.E. Elizondo-Omaña¹ , S. Guzman-Lopez¹ 

¹Human Anatomy Department, School of Medicine, Universidad Autónoma de Nuevo León, Monterrey, Nuevo León, Mexico

²Radiology and Imaging Department, University Hospital “Dr. José Eleuterio González”, Universidad Autónoma de Nuevo León, Monterrey, Nuevo León, Mexico

[Received: 18 October 2022; Accepted: 14 November 2022; Early publication date: 30 November 2022]

Background: The study of the tentorial notch can improve the understanding of brain injury mechanisms. Tentorial morphology has been analysed primarily in cadaveric studies. However, the postmortem effect can cause variability in the measurements. The objective was to evaluate the morphometry of the tentorial notch and the third cranial nerve on living subjects using magnetic resonance imaging (MRI).

Materials and methods: A retrospective cross-sectional study was performed. Using consecutive cases, 60 MRI scans were analysed for tentorial notch morphology. Maximum notch width (MNW), notch length (NL), interpedunculoclival (IC) distance, apicotectal (AT) distance, third cranial nerve (CN-III) distance, and inter-CN-III angle, were obtained. For the classification of the tentorial notch quartile distribution technique for MNW, NL, AT distance, and IC distance were used.

Results: According to the quartile of the MNW, patients were stratified into narrow, midrange, and wide groups. Using the NL quartile groups, they were also classified as short, midrange, and long. With these, the tentorial notch could be classified into eight types. Statistical differences between genders in the MNW and inter-CN-III angle were found, as well as a strong positive correlation between NL and AT distance, and between right and left CN-III distances.

Conclusions: There were differences between the cadaveric samples and living subjects in the CN-III distances. This difference could be explained by the dehydration of brain volume in the postmortem process which may cause nerve elongation. Morphometry of the tentorial notch and its neurovascular relations allows a better understanding of the mechanisms of brain herniation. (Folia Morphol 2023; 82, 4: 784–790)

Key words: tentorial notch, third cranial nerve, brainstem, brain herniation

Address for correspondence: Dr. S. Guzman-Lopez and Dr. R.E. Elizondo-Omaña, Facultad de Medicina, Universidad Autónoma de Nuevo León, Av. Madero and Dr. Aguirre Pequeño S/N, Col. Mitras Centro, C.P. 64460, Monterrey, Nuevo León, México, tel: +52 1 81 8329 4171, fax: +521 81 8347 7790, e-mail: dr.santos.anato@gmail.com; rod_omana@yahoo.com

*Both authors participated equally in the study and are both in the position of first author.

This article is available in open access under Creative Common Attribution-Non-Commercial-No Derivatives 4.0 International (CC BY-NC-ND 4.0) license, allowing to download articles and share them with others as long as they credit the authors and the publisher, but without permission to change them in any way or use them commercially.

INTRODUCTION

The cerebellar tentorium is a semilunar-shaped extension of the dura mater that separates the cerebellum from the cerebral hemispheres [17]. The triangular-shaped aperture located between the free edges of the tentorium cerebelli and the clivus is defined as the tentorial notch [18]. This space is involved in different brain injury processes due to the relation with midline structures and the rigidity of the dura mater [10].

Tentorial herniation is an upper or lower displacement of the temporal lobe through the tentorial notch, and is one of the most common herniation secondary result of an intracranial mass [15]. Different studies have published the possible influence of the morphometric analysis of this aperture in the understanding of the mechanism of different brain injuries [1, 5, 6]. The patterns of the tentorial herniation and differences in the clinical presentation could be partially influenced by the dimensions of the tentorial notch and the position of the brainstem, but this remains unclear [5].

The morphometric analysis of the tentorial notch has been analysed mainly in cadaveric studies [1, 6, 16, 23]. However, the tissue deterioration in the postmortem process, alterations due to dehydration from the absence of circulation, and the method of conservation used could have an impact on measurements, varying amongst themselves [7, 25, 27]. The objective of this study is to evaluate the morphometry of the tentorial notch and the third cranial nerve (CN-III) in living subjects by magnetic resonance imaging (MRI).

MATERIALS AND METHODS

A retrospective cross-sectional study was performed with 60 Fast Imaging Employing Steady/State Acquisition (FIESTA) MRI sequences. The study images were obtained from the database of the Radiology and Imaging Department. Screening was consecutive cases of patients between 18 and 60 years who underwent a brain FIESTA MRI sequence indicated by their treating physician. We excluded patients with posterior fossa diseases, central nervous system vascular disease, previous cranial surgery, or other central nervous system diseases that may alter anatomy. Studies with abnormalities or artifacts were eliminated. This study adheres to the STROBE guidelines for the report of observational studies [26].

Study technique

All patients underwent a head FIESTA MRI sequence (3 Tesla, Signa Twin HDx of General Electric-GE), Software 5.7.1, using the following parameters — temporal resolution: 1000 ms, echo time: 136 ms, flip angle: 110°, slice-thickness: 0.6 mm, slice oversampling: field of view: 200 × 200 mm, matrix: 320 × 320. All the imaging data was uploaded to the Carestream Vue PACS and analysed in coronal, axial, and sagittal planes. The images and measurements were assessed independently by two neuro-radiologists recorded in a database using millimetres with two decimal unit precision. All sets of inter-observer reliability analyses resulted in substantial reliability (interclass coefficient > 0.85 and Cohen's kappa > 0.85).

Tentorial notch measurements

Definition and anatomical fundamentals for interpretation of the tentorial notch and CN-III variables, have been described mainly in human cadaveric samples. However, Adler et al. [1] reported a method to measure these variables using MRI. The following variables were measured: maximum notch width (MNW), notch length (NL), interpedunculoclival (IC) distance, and apicotectal (AT) distance. Although the anterior notch width, defined as the width of the tentorial notch in the dorsum sellae, is a variable described by other authors, this could not be reproduced with MRI. We propose a method for studying the CN-III with MRI with the following measures: CN-III distance, and inter-CN-III angle (Fig. 1). Although the measurement may be done by T2 RMI sequence

For the classification of the tentorial notch defined by Adler et al. [1] quartile distribution technique for MNW, NL, AT distance, and IC distance was used. Using the MNW quartile distribution the tentorial notch was divided into narrow, midrange, and long. The NL and AT distances quartile distribution were used to classify into short, midrange, and long. The position of the brainstem within the tentorial notch was labelled as pre-fixed, mid-position, and post-fixed applying the quartile distribution technique with the IC distance. According to the classification defined by Adler et al. [1] we used the MWN and NL to stratify tentorial notch into 8 types.

Ethical considerations

This study was previously reviewed and approved by the University's Ethics and Research Committees

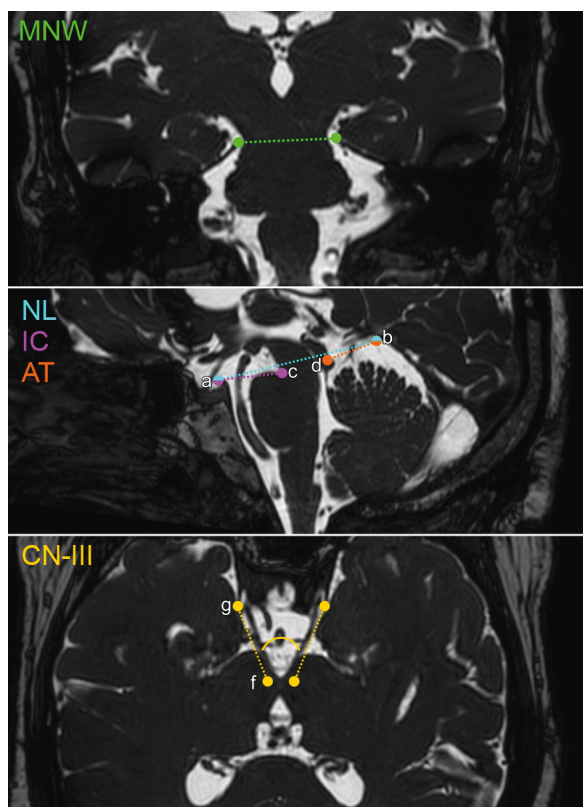


Figure 1. Measurements of the tentorial notch. Maximum notch width (MNW): using a coronal plane, the maximum width between the border of the tentorial notch in the coronal plane. Notch length (NL): using a sagittal plane, the length of the tentorial notch from the superior edge of the dorsum sellae (letter a) to the apex of the tentorial notch (letter b). Interpedunculoclival (IC) distance: using a sagittal plane, the distance between the superior edge of the dorsum sellae to the interpeduncular fossa (letter c). Apicotectal (AT) distance: using a sagittal plane, the distance from the tectum (letter d) to the apex of the tentorial notch. Left and right third cranial nerve (CN-III) distance: using a transverse plane, the distance between the origin of the CN-III (letter f) to the cavernous sinus (letter g). Inter-CN-III angle: using a transverse plane, the angle between the two third cranial nerves (curve line).

with the registration number AH21-00010, making sure it adheres to the Helsinki Declaration and national and international standards of research. The authors declare no financial or commercial gain for the realisation of this study. The authors declare no conflict of interest. None of the imaging studies were performed for the purposes of this study.

Statistical analysis

Sample size calculation was made with the formula for estimating a mean in an infinite population with a confidence of 95% and a margin of error of 5% resulting in a total of 60 studies. We obtained central tendency and dispersion data of the sample

variables. We performed the Kolmogorov-Smirnov test for normality. Due to the normality distribution of sample data, the comparison between different sexes groups was made with a two-tailed Student t-test. Correlation tests were performed by Pearson correlation coefficients. The 95% confidence interval (CI) was obtained for the mean between-difference. A p-value of < 0.5 was considered statistically significant. For multiple comparisons, the Bonferroni correction was performed to adjust the p-value. The database was analysed using the SPSS Version 25.0 programme for Windows 10 (IBM, Armonk, NY, USA).

RESULTS

Descriptive statistics of the measurements stratified by sex are shown in Table 1. The mean age of the sample was 41.5 ± 12.1 years, of which 36 (60%) were women with a mean age of 42.08 ± 9.23 years and 24 (40%) men with a mean age of 41.11 ± 13.8 years. We found statistically differences between sexes in MNW distance and inter-CN-III angle. The MNW mean is 32.13 mm (range 28.1–39.8, 95% CI 30.95–33.31) for men and 30.72 mm (range 28.1–39.8, 95% CI 29.89–31.56) for women. The mean between-group difference is 1.4 mm (95% CI 0.038–2.77; $p = 0.04$). The inter-CN-III angle mean is 56.72 grades (range 45.72–70.56, 95% CI 53.98–59.46) for man and 53 grades (range 41.78–71.24, 95% CI 50.69–55.32). The mean between-group difference is of 3.71 grades (95% CI 0.20–7.22; $p = 0.04$).

Pearson's correlation coefficient between variables is shown in Table 2. We found a strong positive correlation coefficient between measurements between NL and AT distance ($r = 0.78$; $r^2 = 0.62$), and between right and left CN-III distances ($r = 0.93$; $r^2 = 0.86$).

Table 3 shows the ranges of the measurements used to classify the tentorial notch using MNW and NL quartiles and the percentages of the different types. The typical type that corresponds to the MNW and NL midrange was the most common. The mixed type was the least frequent in this sample.

DISCUSSION

Main findings

This study analysed the morphology of the tentorial notch and CN-III on living subjects in a healthy population. Our study demonstrates consistency with cadaveric studies, except for the variables of the CN-III. We obtained statistically significant differences between sexes in MNW and inter-CN-III angle; how-

Table 1. Comparison measurements of the tentorial notch between sexes

| Measurement | General (n = 60) | Women (n = 36) | Men (n = 24) | P |
|---------------------------------|------------------|----------------|--------------|-------|
| Maximum notch width | 31.28 ± 2.66 | 30.72 ± 2.46 | 32.13 ± 2.78 | 0.04* |
| Notch length | 55.55 ± 4.82 | 55.94 ± 4.94 | 54.98 ± 4.66 | 0.45 |
| Apicotectal distance | 19.45 ± 3.81 | 19.8 ± 3.95 | 18.93 ± 3.6 | 0.39 |
| Interpedunculoclival distance | 21.03 ± 3.17 | 20.93 ± 3.32 | 21.17 ± 2.98 | 0.78 |
| Right cisternal CN-III distance | 22.81 ± 4.11 | 23.99 ± 3.81 | 22.03 ± 4.17 | 0.07 |
| Left cisternal CN-III distance | 22.02 ± 3.96 | 22.71 ± 3.76 | 21.56 ± 4.08 | 0.27 |
| Inter-CN-III angle | 54.49 ± 6.89 | 56.72 ± 6.49 | 53 ± 6.84 | 0.04* |

Data are shown as mean ± standard deviation. Values are expressed in millimetres for distances and grades for angles. Independent-sample Student t-test was used for compared measurements between sexes; *statistically significant ($p < 0.05$); CN-III — third cranial nerve

Table 2. Pearson's correlation coefficient between measurements of the tentorial notch

| | MNW | NL | AT distance | IC distance | Right CN-III distance | Left CN-III distance |
|-----------------------|-----|-------|-------------|-------------|-----------------------|----------------------|
| MNW | | 0.227 | 0.239 | -0.056 | 0.456* | 0.374* |
| NL | | | 0.788* | 0.482* | 0.401 | 0.479* |
| AT distance | | | | 0.056 | 0.208 | 0.267 |
| IC distance | | | | | 0.286 | 0.297* |
| Right CN-III distance | | | | | | 0.935* |
| Left CN-III distance | | | | | | |

*Statistically significant with Bonferroni correction; AT — apicotectal; CN-III — third cranial nerve; IC — interpedunculoclival; MNW — maximum notch width; NL — notch length

Table 3. Types of tentorial notch

| Type of notch | Dimension | Range [mm] | Percentage |
|---------------|----------------|------------|------------|
| Wide | MNW (wide) | 32.5–39.8 | 15% |
| | NL (midrange) | 55.6–58.9 | |
| Narrow | MNW (narrow) | 26.5–29.5 | 11.6% |
| | NL (midrange) | 55.6–58.9 | |
| Long | MNW (midrange) | 29.6–32.4 | 10% |
| | NL (long) | 59–64.9 | |
| Short | MNW (midrange) | 29.6–32.4 | 15% |
| | NL (short) | 46.6–55.5 | |
| Typical | MNW (midrange) | 29.6–32.4 | 25% |
| | NL (midrange) | 55.6–58.9 | |
| Large | MNW (wide) | 32.5–39.8 | 10% |
| | NL (long) | 59–64.9 | |
| Small | MNW (narrow) | 26.5–29.5 | 10% |
| | NL (short) | 46.6–55.5 | |
| Mixed | MNW (narrow) | 26.5–29.5 | 3% |
| | NL (long) | 59–64.9 | |
| | MNW (wide) | 32.5–39.8 | 0% |
| | NL (short) | 46.6–55.5 | |

MNW — maximum notch width; NL — notch length

ever, the absolute difference was small. Currently, a distinction between sexes in the understanding

of brain injury has not been established. A strong positive correlation was found between NL and AT distance, and between the right and left cisternal CN-III distance.

Comparison with other studies

Most studies regarding tentorial notch analysis have used cadavers, which carries an important limitation (Table 4) [1, 6, 16, 23]. In the cadaveric conservation process, the deep brain is the last part conserved, as the fixation agent spread from the surface of the brain [7]. The conservation process depends mainly on the time of the initiation of the procedure after death [7, 9]. This allows macroscopic changes in the brain to set in, as the putrefaction phase of the postmortem process can be seen as early as 24 hours succeeding the death, which may impact on the measurements [14].

We obtained similar results in the MNW and NL measurements compared with other populations [1, 6, 16, 20, 22, 23]. Adler et al. [1] studied a larger population than other studies but the mean and standard deviation are similar among authors (Table 4). The variables that include dura matter appear to be less affected by the postmortem process than other structures inside the head [3].

Table 4. Measurement comparison of the tentorial notch between other populations

| Author | Arrambide-Garza et al., 2022 | Das et al., 2021 [6] | Staquet et al., 2020 [22] | Adler et al., 2002 [1] | Sunderland et al., 1984 [23] | Ono et al., 1984 [16] |
|-----------------------|------------------------------|----------------------|---------------------------|------------------------|------------------------------|-----------------------|
| Country | Mexico | USA | France | USA | Australia | USA |
| Sample | 60 MRIs | 40 cadavers | 40 CTs | 110 cadavers | 30 cadavers | 25 cadavers |
| Age | 41.5 ± 12.1 | 20 to 65 | – | 42.5 | – | – |
| ANW | – | 26.92 ± 2.14 | 25.5 ± 3.5 | 26.6 ± 2.7 | 27.06 ± 3.5 | – |
| MNW | 31.28 ± 2.66 | 29.77 ± 2.26 | 31.0 ± 2.5 | 29.6 ± 3.0 | 30.16 ± 3.21 | 29.6 (26–35) |
| NL | 55.55 ± 4.82 | 57.98 ± 4.52 | 55.0 ± 5.3 | 57.7 ± 5.6 | 54.9 ± 6.93 | 52 (46–67) |
| IC distance | 21.03 ± 3.17 | 21.21 ± 3.72 | – | 20.4 ± 3.2 | – | 12.1 (7.8–15.6) |
| AT distance | 19.45 ± 3.81 | 25.81 ± 8.04 | – | 16.8 ± 5.4 | – | 19.8 (13–27) |
| Right CN-III distance | 22.81 ± 4.11 | – | – | 26.1 ± 3.2 | – | – |
| Left CN-III distance | 22.02 ± 3.96 | – | – | 26.7 ± 2.9 | – | – |
| Inter-CN-III angle | 54.49 ± 6.89 | – | – | 57.3 ± 7.3 | – | – |

Data are shown as mean ± standard deviation and mean (range). Values are expressed in millimetres for distances and grades for angles. ANW — anterior notch width; AT — apicortical; CN-III — third cranial nerve; CT — computed tomography; IC — interpedunculoval; MRI — magnetic resonance imaging; MNW — maximum notch width; NL — notch length

The tentorial notch is divided into the anterior, middle, and posterior incisural spaces depending on the relation with the brainstem [4, 21]. The anterior and posterior incisural spaces are located anterior and posterior to the brainstem, respectively [18]. The anterior incisural space contains the internal carotid artery, basilar artery, optic nerves, and CN-III [23]. Despite the differences between the types of samples, we obtained similar results in the IC distance to Adler et al. (21.03 mm) [1] and Das et al. (21.21 mm) [6] but different results than Ono et al. (12.1 mm) [16]. The posterior incisura space lies posterior to the brainstem and contains the posterior cerebral artery, superior cerebellar artery, the internal and basal vein, and the fourth cranial nerve [18]. We found similar results to Adler et al. (16.8 mm) [1] and Ono et al. (19.8 mm) [16] but different data than to Das et al. (25.81 mm) [6]. These differences between cadaveric studies could be explained by the conservation method used and the population studied.

The CN-III exits from the midbrain and passes through the cavernous sinus, prior to entering the orbit through the supraorbital fissure [12]. We studied the distance of the CN-III from its origin to the cavernous sinus with differences in the length (right: 22.81 mm, left: 22.02 mm) compared to Adler et al. (right: 26.1 mm, left: 26.7 mm) [1]. However, results were similar in the inter CN-III (54.49 vs. 57.3 grades). The difference in the length of the CN-III could be explained by the dehydration of the brain in the postmortem process, causing an elongation of the nerve.

Brain herniation

Brain herniation is the most common secondary result of an intracranial mass. It is defined as a displacement of cerebral tissue from a compartment to another [19]. Clinical presentation varies according to the compartment and the brain structure affected. The tentorial herniation could cause pupillary dilatation, ophthalmoplegia, or ipsilateral hemiplegia due to the compression of the brainstem and CN-III [24]. Despite the actual comprehension of the mechanism of the tentorial herniation, the reason for the clinical variation among patients is still unclear. The severity of the disease is determined mainly by the volume of the mass lesion, the localization, or the velocity of the pathological process [11]. In addition, the dimensions of the tentorial notch could have an implication on the clinical and severity of the brain herniation in patients with the same type of lesion [5, 23].

The anterior incisura space is a site where the temporal lobe could move and compress the CN-III and cerebral peduncles during the tentorial herniation [6]. The length of the anterior incisural space could be estimated with the IC distance. Patients with wider and longer notches could have more exposition of the posterior cranial fossae and facilitate the displacement of the brain in the herniation process.

The superior aspect of the cerebellum is related to the posterior incisural space [18]. Although the cerebellar tissue exposed through the posterior incisural space could not be studied by MRI, it could be estimated by the AT distance [6]. The relation between large apertures and the total of the cerebellar tissue

exposed has been described in cadaveric studies. The cerebellar tissue has a higher exposition in a long and wide tentorial notch than in a short and narrow notch. These findings could influence the cerebellar herniation through the tentorial notch [1, 13, 23].

The length and course of the CN-III may be an explanation for the clinical differences among patients with this pathology. The tentorial herniation compresses mainly the brainstem and (CN-III) during the movement of the temporal lobe through the tentorial notch [2, 8].

The MWN and NL are used to stratify the tentorial notch into 8 types. Grille et al. [11] studied the characteristics of the tentorial notch in neurocritical patients. They described the “narrow,” “short,” and “small” as the most common types in neurocritical patients, which corresponded to wider and longer notch types [11]. Further studies comparing the characteristics in neurocritical patients are needed to determine the association between tentorial notch types and herniation patterns.

Limitations of the study

Our study has several limitations. Although the sample size was calculated to determine statistical difference, larger samples are needed to make a comparison between different populations. The measurements of the CN-III have not been validated by other studies or compared with other radiology techniques. The patients’ anthropometric characteristics were not included in the analysis. The study was conducted using Hispanic patients; however further data is needed to compare results with other populations. Grille et al. [11] validated the MRI and computed tomography, but the brainstem and CN-III cannot be studied using computed tomography. Our study used MRI with FIESTA sequence, which is not broadly available.

CONCLUSIONS

Changes in cadaveric models in the tentorial notch could have an impact on the morphology of the tentorial notch and its neurovascular relations. There were differences between the cadaveric samples and living subjects in the cisternal third nerve distances. This difference could be explained by the dehydration of the brain in the postmortem process which may cause nerve elongation. The measurements of the tentorial notch may have implications for a better understanding of the mechanisms of brain herniation.

Conflict of interest: None declared

REFERENCES

1. Adler DE, Milhorat TH. The tentorial notch: anatomical variation, morphometric analysis, and classification in 100 human autopsy cases. *J Neurosurg.* 2002; 96(6): 1103–1112, doi: [10.3171/jns.2002.96.6.1103](https://doi.org/10.3171/jns.2002.96.6.1103), indexed in Pubmed: [12066913](https://pubmed.ncbi.nlm.nih.gov/12066913/).
2. Angulo Carvallo N, Patil P, Abello AL. Cerebral herniation. *Crit Find Neuroradiol.* 2016: 13–19, doi: [10.1007/978-3-319-27987-9_2](https://doi.org/10.1007/978-3-319-27987-9_2).
3. Bliss LA, Sams MR, Deep-Soboslay A, et al. Use of post-mortem human dura mater and scalp for deriving human fibroblast cultures. *PLoS One.* 2012; 7(9): e45282, doi: [10.1371/journal.pone.0045282](https://doi.org/10.1371/journal.pone.0045282), indexed in Pubmed: [23028905](https://pubmed.ncbi.nlm.nih.gov/23028905/).
4. Bull JW. Tentorium cerebelli. *Proc R Soc Med.* 1969; 62(12): 1301–1310, doi: [10.1177/003591576906201242](https://doi.org/10.1177/003591576906201242), indexed in Pubmed: [4983118](https://pubmed.ncbi.nlm.nih.gov/4983118/).
5. Corsellis JA. Individual variation in the size of the tentorial opening. *J Neurol Neurosurg Psychiatry.* 1958; 21(4): 279–283, doi: [10.1136/jnnp.21.4.279](https://doi.org/10.1136/jnnp.21.4.279), indexed in Pubmed: [13611569](https://pubmed.ncbi.nlm.nih.gov/13611569/).
6. Das A, Chhabra S, Das S, et al. The tentorial notch: morphometric analysis and its clinical relevance to neurosurgery. *J Clin Diagn Res.* 2021, doi: [10.7860/jcdr/2021/47758.14545](https://doi.org/10.7860/jcdr/2021/47758.14545).
7. Dawe RJ, Bennett DA, Schneider JA, et al. Postmortem MRI of human brain hemispheres: T2 relaxation times during formaldehyde fixation. *Magn Reson Med.* 2009; 61(4): 810–818, doi: [10.1002/mrm.21909](https://doi.org/10.1002/mrm.21909), indexed in Pubmed: [19189294](https://pubmed.ncbi.nlm.nih.gov/19189294/).
8. Fisher CM. Brain herniation: a revision of classical concepts. *Can J Neurol Sci.* 1995; 22(2): 83–91, doi: [10.1017/s0317167100040142](https://doi.org/10.1017/s0317167100040142), indexed in Pubmed: [7627921](https://pubmed.ncbi.nlm.nih.gov/7627921/).
9. Fountoulakis M, Hardmeier R, Höger H, et al. Postmortem changes in the level of brain proteins. *Exp Neurol.* 2001; 167(1): 86–94, doi: [10.1006/exnr.2000.7529](https://doi.org/10.1006/exnr.2000.7529), indexed in Pubmed: [11161596](https://pubmed.ncbi.nlm.nih.gov/11161596/).
10. Glaister J, Carass A, Pham DL, et al. Automatic falx cerebri and tentorium cerebelli segmentation from magnetic resonance images. *Proc SPIE Int Soc Opt Eng.* 2017; 10137, doi: [10.1117/12.2255640](https://doi.org/10.1117/12.2255640), indexed in Pubmed: [28943701](https://pubmed.ncbi.nlm.nih.gov/28943701/).
11. Grille P, Biestro A, Telis O, et al. Individual variation of tentorial notch morphometry in a series of neurocritical patients. *Arq Neuropsiquiatr.* 2021; 79(9): 781–788, doi: [10.1590/0004-282X-anp-2020-0335](https://doi.org/10.1590/0004-282X-anp-2020-0335), indexed in Pubmed: [34669814](https://pubmed.ncbi.nlm.nih.gov/34669814/).
12. Heiland Hogan MB, Subramanian S, Das JM. Neuroanatomy, Edinger–Westphal Nucleus (Accessory Oculomotor Nucleus). StatPearls Publishing, Treasure Island (FL) 2022.
13. Klintworth GK. The comparative anatomy and phylogeny of the tentorium cerebelli. *Anat Rec.* 1968; 160(3): 635–642, doi: [10.1002/ar.1091600312](https://doi.org/10.1002/ar.1091600312), indexed in Pubmed: [5664078](https://pubmed.ncbi.nlm.nih.gov/5664078/).
14. Mann RW, Bass WM, Meadows L. Time since death and decomposition of the human body: variables and observations in case and experimental field studies. *J Forensic Sci.* 1990; 35(1): 103–111, indexed in Pubmed: [2313251](https://pubmed.ncbi.nlm.nih.gov/2313251/).
15. Munakomi S, Das JM. Brain herniation. StatPearls Publishing, Treasure Island (FL) 2022.
16. Ono M, Ono M, Rhoton AL, et al. Microsurgical anatomy of the region of the tentorial incisura. *J Neurosurg.* 1984;

- 60(2): 365–399, doi: [10.3171/jns.1984.60.2.0365](https://doi.org/10.3171/jns.1984.60.2.0365), indexed in Pubmed: [6693964](https://pubmed.ncbi.nlm.nih.gov/6693964/).
17. Rai R, Iwanaga J, Shokouhi G, et al. The tentorium cerebelli: a comprehensive review including its anatomy, embryology, and surgical techniques. *Cureus*. 2018; 10(7): e3079, doi: [10.7759/cureus.3079](https://doi.org/10.7759/cureus.3079), indexed in Pubmed: [30305987](https://pubmed.ncbi.nlm.nih.gov/30305987/).
 18. Rhoton AL. Tentorial incisura. *Neurosurgery*. 2000; 47(3 Suppl): S131–S153, doi: [10.1097/00006123-200009001-00015](https://doi.org/10.1097/00006123-200009001-00015), indexed in Pubmed: [10983307](https://pubmed.ncbi.nlm.nih.gov/10983307/).
 19. Riveros Gilardi B, Muñoz López JI, Hernández Villegas AC, et al. Types of cerebral herniation and their imaging features. *Radiographics*. 2019; 39(6): 1598–1610, doi: [10.1148/rg.2019190018](https://doi.org/10.1148/rg.2019190018), indexed in Pubmed: [31589570](https://pubmed.ncbi.nlm.nih.gov/31589570/).
 20. Salinas-Alvarez Y, Arrambide-Garza F, Elizondo-Omaña R, et al. Morphometric analysis of the tentorial notch by magnetic resonance. *FASEB J*. 2022; 36(S1), doi: [10.1096/fasebj.2022.36.s1.r2423](https://doi.org/10.1096/fasebj.2022.36.s1.r2423).
 21. Samii M, Carvalho GA, Tatagiba M, et al. Meningiomas of the tentorial notch: surgical anatomy and management. *J Neurosurg*. 1996; 84(3): 375–381, doi: [10.3171/jns.1996.84.3.0375](https://doi.org/10.3171/jns.1996.84.3.0375), indexed in Pubmed: [8609546](https://pubmed.ncbi.nlm.nih.gov/8609546/).
 22. Staquet H, Francois PM, Sandoz B, et al. Surface reconstruction from routine CT-scan shows large anatomical variations of falx cerebri and tentorium cerebelli. *Acta Neurochir (Wien)*. 2021; 163(3): 607–613, doi: [10.1007/s00701-020-04256-2](https://doi.org/10.1007/s00701-020-04256-2), indexed in Pubmed: [32034496](https://pubmed.ncbi.nlm.nih.gov/32034496/).
 23. Sunderland S. The tentorial notch and complications produced by herniations of the brain through that aperture. *Br J Surg*. 1958; 45(193): 422–438, doi: [10.1002/bjs.18004519306](https://doi.org/10.1002/bjs.18004519306), indexed in Pubmed: [13536343](https://pubmed.ncbi.nlm.nih.gov/13536343/).
 24. Tadevosyan A, Kornbluth J. Brain herniation and intracranial hypertension. *Neurol Clin*. 2021; 39(2): 293–318, doi: [10.1016/j.ncl.2021.02.005](https://doi.org/10.1016/j.ncl.2021.02.005), indexed in Pubmed: [33896520](https://pubmed.ncbi.nlm.nih.gov/33896520/).
 25. Tapia-Nañez M, Quiroga-Garza A, Guerrero-Mendivil F, et al. A review of the importance of research in Anatomy, an evidence-based science. *Eur J Anat*. 2022; 26(4), doi: [10.52083/EVZA1394](https://doi.org/10.52083/EVZA1394).
 26. von Elm E, Altman DG, Egger M, et al. STROBE Initiative. The Strengthening the Reporting of Observational Studies in Epidemiology (STROBE) statement: guidelines for reporting observational studies. *Bull World Health Organ*. 2007; 85(11): 867–872, doi: [10.2471/blt.07.045120](https://doi.org/10.2471/blt.07.045120), indexed in Pubmed: [18038077](https://pubmed.ncbi.nlm.nih.gov/18038077/).
 27. Weickenmeier J, Kurt M, Ozkaya E, et al. Brain stiffens post mortem. *J Mech Behav Biomed Mater*. 2018; 84: 88–98, doi: [10.1016/j.jmbbm.2018.04.009](https://doi.org/10.1016/j.jmbbm.2018.04.009), indexed in Pubmed: [29754046](https://pubmed.ncbi.nlm.nih.gov/29754046/).